

Autophosphorylation of FGFR1 Kinase Is Mediated by a Sequential and Precisely Ordered Reaction

Short Article

Cristina M. Furdai,^{1,2} Erin D. Lew,^{1,2}
Joseph Schlessinger,^{1,*} and Karen S. Anderson^{1,*}

¹Department of Pharmacology
Yale University School of Medicine
New Haven, Connecticut 06520

Summary

Tyrosine phosphorylation of cellular proteins induced by extracellular cues serves as a critical mediator in the control of a great variety of cellular processes. Here, we describe an integrated experimental approach including rapid quench methodology and ESI-LC-MS/MS as well as time-resolved ESI-MS to demonstrate that tyrosine autophosphorylation of the catalytic tyrosine kinase domain of FGF-receptor-1 (FGFR1) is mediated by a sequential and precisely ordered reaction. We also demonstrate that the rate of catalysis of two FGFR substrates is enhanced by 50- to 100-fold after autophosphorylation of Y653 in the activation loop, whereas autophosphorylation of the second site in the activation loop (Y654) results in 500- to 1000-fold increase in the rate of substrate phosphorylation. We propose that FGFR1 is activated by a two-step mechanism mediated by strictly ordered and regulated autophosphorylation, suggesting that distinct phosphorylation states may provide both temporal and spatial resolution to receptor signaling.

Introduction

A wealth of information on the cellular and molecular biology of signal transduction pathways mediated by receptor tyrosine kinases (RTKs) has become available over the last two decades, with an emphasis on delineating plausible cell signaling pathways and identifying signaling partners (Schlessinger, 2000; Blume-Jensen and Hunter, 2001; Pawson and Nash, 2003). More recently, several of the signaling networks for RTK pathways have been the subject of a series of quantitative proteomic experiments with mass spectrometry to examine these events in a time-resolved manner (Blagoev et al., 2004; Johnson and Hunter, 2004; Zhang et al., 2005). Collectively, studies examining the overall temporal changes for specific activation of RTKs have revealed that different proteins are recruited and distinct signaling pathways are stimulated over a time continuum rather than via a simple binary system for pathway activation (Steen et al., 2002; Blagoev et al., 2004; Hinsby et al., 2003). A more detailed level of control might suggest that different kinetics of autophosphorylation of different tyrosine residues may lead to a distinct activation pattern of downstream effector proteins. Therefore, combining structural information of RTKs with the dynamics of receptor autophosphorylation may provide in-

sights into our understanding of how the activities of RTKs are regulated. Rapid chemical quench and stopped-flow fluorescence methodologies (Johnson, 2003) are proven approaches to reveal the kinetic profile and the temporal events at the enzyme active site. More recent and complementary methods utilizing rapid-mixing/time-resolved, high-resolution mass spectrometry (Li et al., 2003, 2005) provide the ability to map in real time the creation and dynamic order of new molecular species along the reaction pathway. Together, these methods provide a powerful approach to define a comprehensive mechanistic understanding of the catalytic mechanism of RTKs.

The fibroblast growth factor receptor (FGFR) family consists of four RTKs composed of an extracellular ligand binding domain, a single transmembrane spanning region, and an intracellular cytoplasmic portion containing a protein tyrosine kinase core. Upon costimulation by FGFs together with heparin or heparan sulfate proteoglycan, FGFRs undergo dimerization and transautophosphorylation on critical tyrosine residues in the cytoplasmic domain, most of which are conserved among the FGFR family members. It has been shown that autophosphorylation of tyrosines in the activation loop of the protein tyrosine kinase (PTK) domain is critical for maintaining the PTK in an active state (Mohammadi et al., 1996a). Tyrosine autophosphorylation of other tyrosine residues in the cytoplasmic domain is essential for recruitment and activation of downstream signaling partners, which participate in the regulation of diverse processes such as cell growth and differentiation, cell metabolism, and cell survival (reviewed in Eswarakumar et al. [2005]). Aberrant FGF signaling has been implicated in multiple human skeletal dysplasias and in different cancers (Eswarakumar et al., 2005; Grose and Dickson, 2005). Thus, autophosphorylation of FGFR1 as well as other RTKs regulates both the catalytic activity of the tyrosine kinase and the subsequent initiation of downstream signaling events.

In this report, we apply a comprehensive experimental approach based upon rapid chemical quench and mass spectrometry to explore the autophosphorylation of the PTK domain of FGFR1 (FGFR1K). We demonstrate that the five tyrosine autophosphorylation sites in the catalytic core of FGFR1 are phosphorylated by a precisely controlled and ordered reaction. We also demonstrate that the rate of catalysis of two substrates is enhanced by 50- and 500-fold after autophosphorylation of Tyr653 and Tyr654, respectively, in the activation loop of FGFR1. These experiments show that FGFR1 is autophosphorylated by a strictly ordered reaction, suggesting that, within a defined time window, different signaling pathways may be recruited and activated.

Results and Discussion

We have performed a detailed analysis of FGFR1K autophosphorylation by using an integrated experimental approach that includes rapid chemical quench methodology coupled with LC/ESI-MS/MS and time-resolved

*Correspondence: joseph.schlessinger@yale.edu (J.S.); karen.anderson@yale.edu (K.S.A.)

²These authors contributed equally to this work.

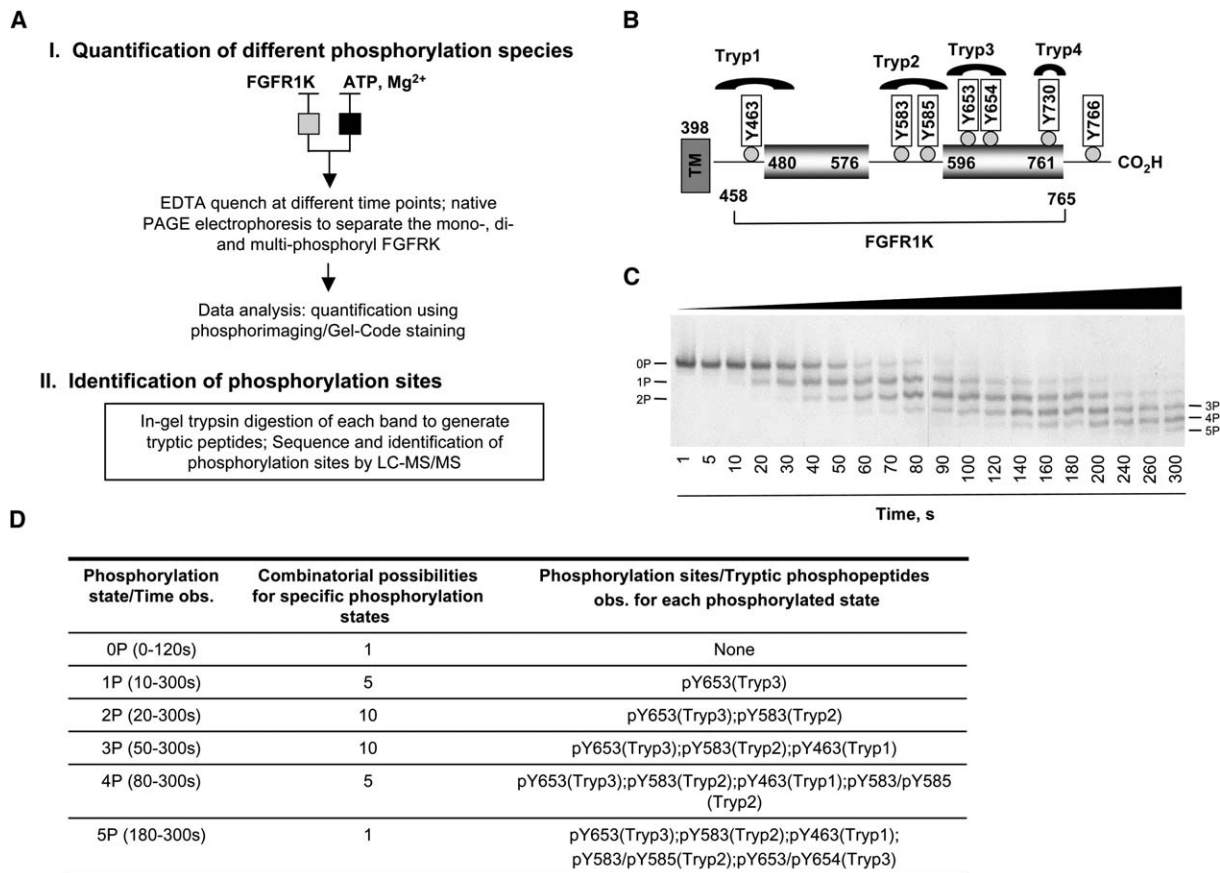


Figure 1. Quantitative Analysis of FGFR1K Autophosphorylation

(A) Experimental strategy for the quantification of different phosphorylated species and identification of phosphorylation sites.

(B) A diagram of FGFR1K describing the position of the tyrosine autophosphorylation sites. Tryp1 to Tryp4 represent tryptic peptides from FGFR1K containing the tyrosine autophosphorylation sites.

(C) Progression of FGFR1K autophosphorylation revealed by native PAGE analysis. FGFR1K (35 μ M) was reacted with 5 mM ATP and 10 mM MgCl₂ in a rapid chemical quench apparatus as described in the [Experimental Procedures](#). The phosphorylation states at each time point were separated by native PAGE electrophoresis.

(D) Table summarizing the observed phosphorylation states, the theoretical calculation of the combinatorial possibilities for each specific phosphorylation states, and the tyrosine sites undergoing autophosphorylation along with the respective tryptic peptides. The amino acid sequence of the peptides containing the potential tyrosine phosphorylation sites along with the relevant MS/MS fragment ions is summarized in [Table S1](#).

ESI-TOF MS. Using these approaches, we have examined the possibility of whether autophosphorylation of FGFR1K is mediated in a sequential and time-dependent fashion. Is autophosphorylation of the five tyrosines in the kinase domain mediated by a random process, or do discrete and unique sets of defined mono-, di-, and multiphosphorylated species exist that may function as molecular switches to recruit downstream effectors in an orchestrated manner? An insight linking the structural information of FGFR1K ([Mohammadi et al., 1996b](#)) and the dynamics of autophosphorylation may provide significant contribution to our understanding of how this class of cell receptors mediates their cellular responses.

Our previous mapping experiments have identified tyrosine residues 463, 583, 585, 653, 654, 730, and 766 as the major autophosphorylation sites of FGFR1 both in vitro and in living cells ([Mohammadi et al., 1991, 1996a](#)). With the exception of pY766, a site that functions as a binding site for the SH2 domain of phospholipase-C γ (PLC γ) ([Mohammadi et al., 1991](#)), and the two autophos-

phorylation sites in the activation loop (Y653/Y654), sites essential for tyrosine kinase activation ([Mohammadi et al., 1996a](#)), the function of the other tyrosine autophosphorylation sites remain unknown. We have previously shown that the stoichiometry of Y730 phosphorylation is much lower than the stoichiometry of the other five tyrosine residues ([Mohammadi et al., 1996a](#)).

The first question addressed is whether autophosphorylation of FGFR1 is mediated via a random or by a time-dependent, sequential process. This issue was examined by using a combination of rapid chemical quench and native PAGE analysis/densitometric analysis ([Figure 1A](#)). The reaction time course for autophosphorylation of the FGFR1K (see [Figure 1B](#)) was determined as shown in [Figure 1C](#). To independently confirm the nature of the species separated by native PAGE analysis, we also analyzed the reaction mixture present at different reaction times by ESI-TOF MS ([Figure 2A](#)). The samples were first exchanged into ammonium acetate, a volatile buffer amenable to ESI-MS, and suitable electrospray conditions were developed

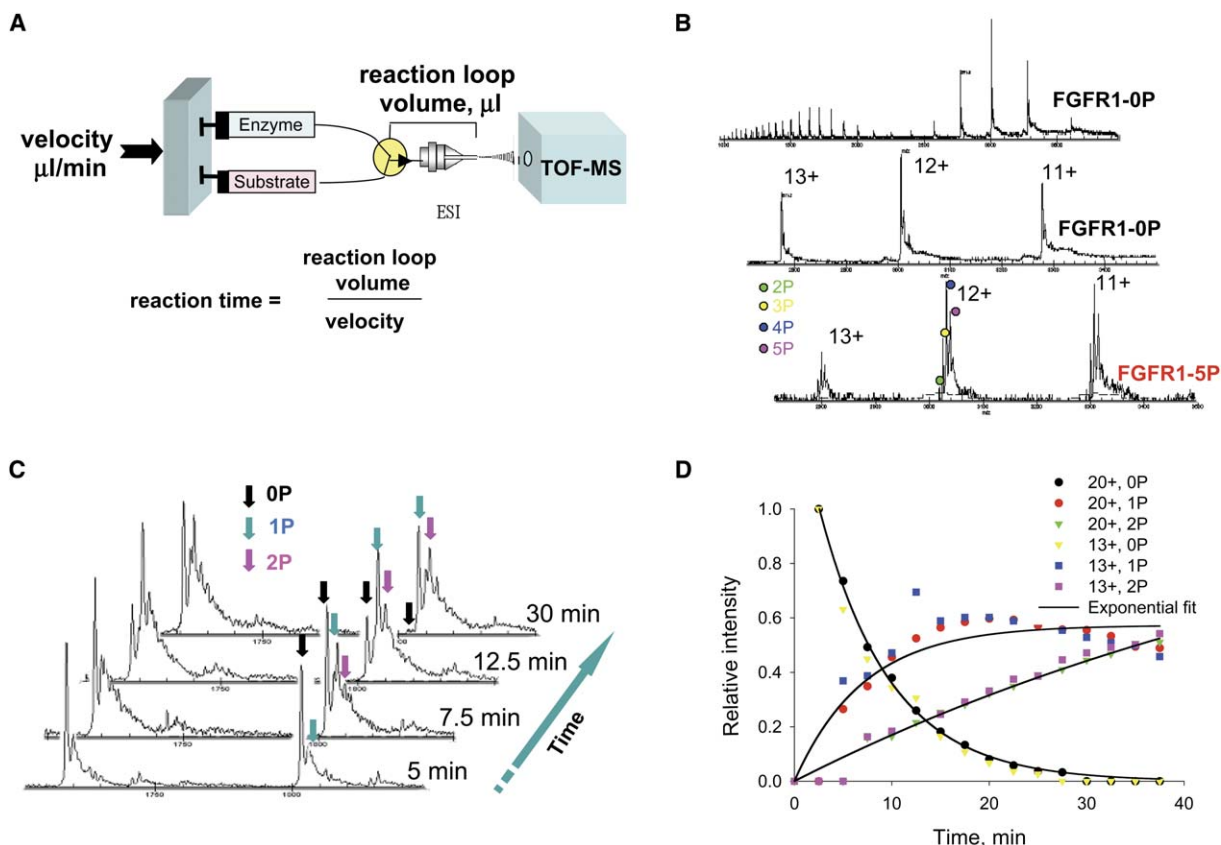


Figure 2. Analysis of FGFR1K Autophosphorylation by Time-Resolved ESI-TOF MS

(A) Instrumental setup for time-resolved ESI-TOF MS.

(B) ESI-TOF MS spectra of the sample quenched at 300 s. ESI-TOF MS spectrum of unphosphorylated FGFR1K showing the full protein envelope (top). ESI-TOF MS spectrum of the unphosphorylated FGFR1K showing the charge states 11+, 12+, and 13+ (middle) and ESI-TOF MS spectrum of the phosphorylated FGFR1K (300 s reaction time) (bottom). Multiple phosphorylated species are present with a relative intensity similar to the native PAGE analysis (last lane, Figure 1C).

(C) A selection of MS spectra collected by time-resolved ESI-TOF MS showing the formation of mono- and diphosphorylated FGFR1K species at increasing reaction times. 0P, 1P, and 2P represent the FGFR1K in unphosphorylated, mono-, and diphosphorylated states.

(D) The relative intensities of unphosphorylated and phosphorylated species are plotted as function of time, and the reaction rates are determined for each phosphorylation event ($0P \rightarrow 1P$, 0.14 min^{-1} and $1P \rightarrow 2P$, 0.013 min^{-1}). 20+ and 13+ indicate data for two different charge states.

to observe the envelope of multiply charged states for protein in the unphosphorylated and fully phosphorylated states, as illustrated in Figure 2B. The ESI-TOF MS analysis coupled with the quench results firmly established that the species separated by native PAGE are indeed multiply phosphorylated FGFR1K and that only five tyrosine residues are phosphorylated. These experiments clearly illustrate that the phosphorylation events occur in a sequential manner and that distinct protein species become phosphorylated as a function of time. In parallel, initial time-resolved ESI-TOF MS experiments were conducted to demonstrate the feasibility of monitoring real-time phosphorylation events by determining the mass of each unphosphorylated and phosphorylated species. We have previously established the quantitative ability of time-resolved ESI-TOF MS to monitor reaction kinetics (Li et al., 2003, 2005). The data in Figure 2C show the time course for the autophosphorylation of FGFR1K at a subsaturating concentration of ATP ($50 \mu\text{M}$). The reaction kinetics quantified by ESI-MS (Figure 2D) are in good agreement with concurrent rapid quench/native PAGE analysis.

The relative abundance of phosphoprotein species present at each time point in the reaction time course shown in Figure 1C was quantified by densitometric analysis and data plotted as a function of time (Figure 3A). KinTekSim modeling of the kinetics was performed based on the mechanism described in Figure 3B. The rate constants for receptor dimerization (k_1) and ATP binding (k_2 , k_4 , k_6 , k_8 , and k_{10}) were 400 and $0.0175 \text{ mM}^{-1}\text{s}^{-1}$, respectively (Figure 3C).

It is well established after more than two decades of research that autophosphorylation of EGFR, FGFR, and other RTKs is mediated by an intermolecular process or, in other words, that the phosphorylation reaction proceeds through a *trans* mechanism (Yarden and Schlessinger, 1987a, 1987b; Honegger et al., 1989; Bellot et al., 1991; Schlessinger, 2000). Subsequent studies confirmed that autophosphorylation reaction of other RTKs is also mediated by an intermolecular process (Cobb et al., 1989; Parast et al., 1998; Murray et al., 2001; Till et al., 2002). A *trans* mechanism would indicate that autophosphorylation reaction of FGFR1K is an intermolecular process and therefore dependent on

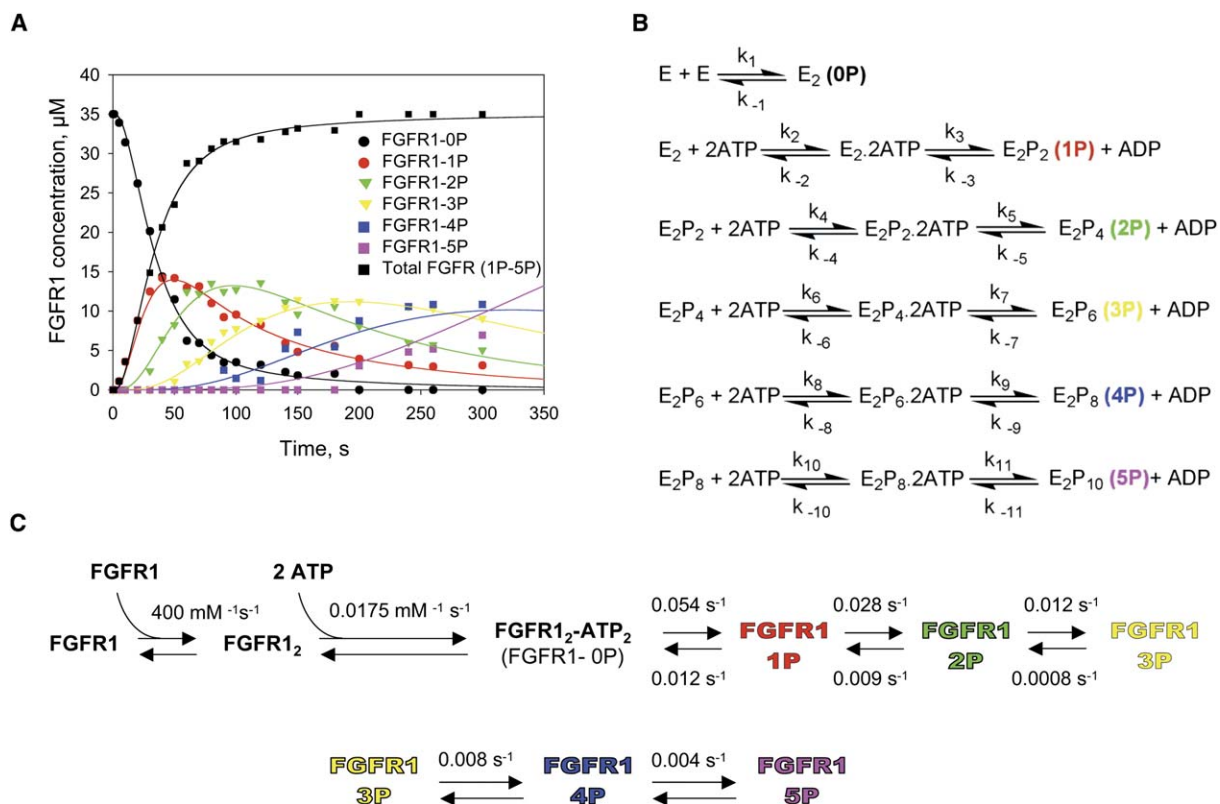


Figure 3. Sequential and Ordered FGFR1K Autophosphorylation

(A) KinTekSim analysis of FGFR1K autophosphorylation. The relative abundance of different phosphorylation states present at each time point were quantified by densitometric analysis and data plotted as function of time. KinTekSim analysis was performed to determine the formation and decay rate of each phosphorylated species according to the reaction mechanism presented in (B): FGFR1K-0P (black), FGFR1K-1P (red), FGFR1K-2P (green), FGFR1K-3P (yellow), FGFR1K-4P (blue), and FGFR1K-5P (magenta).

(B) KinTekSim mechanism showing the dimerization step and the autophosphorylation reaction. The second order rate constants for dimerization (k_1) and ATP binding (k_2 , k_4 , k_6 , k_8 , and k_{10}) were 400 and $0.0175 \text{ mM}^{-1} \text{ s}^{-1}$, respectively. The rate constant for the FGFR1K monophosphorylation (k_3) was 0.054 s^{-1} . The phosphorylation of the subsequent tyrosine residues was increasingly slower, the rate constant being (k_5) 0.028, (k_7) 0.012, (k_9) 0.008, and (k_{11}) 0.004 s^{-1} for the second, third, fourth, and fifth phosphoryl transfer events, respectively.

(C) Simplified reaction scheme illustrating the relevant rates of FGFR1K autophosphorylation.

enzyme concentration. To investigate whether FGFR1K utilized in this system undergoes autophosphorylation via a *cis* or *trans* mechanism, the dependence of the autophosphorylation rate on FGFR1K concentration was analyzed through a series of reactions performed at different protein concentrations ranging from 2.5 to $35 \mu\text{M}$ (Figure S1 available in the Supplemental Data with this article online). The reaction rates for FGFR1K-1P formation obtained from KinTekSim analysis of autophosphorylation reaction at each enzyme concentration were plotted and data analyzed by using a Hill equation. The rate of autophosphorylation was dependent upon protein concentration confirming that autophosphorylation is mediated by a *trans* mechanism that reached saturation at $35 \mu\text{M}$ with a K_d of $5 \mu\text{M}$. We have also investigated the protein concentration dependence for the subsequent phosphorylation steps and found that the second phosphorylation event also takes place in *trans*.

The next question addressed is whether there is heterogeneity in tyrosine autophosphorylation of FGFR1K. As illustrated in the second column of Figure 1D, the combinatorial possibilities suggest that there may be up to ten possible phosphoprotein species (3P or 4P). On the other hand, if tyrosine autophosphorylation of

FGFR1K is homogenous, a discrete, unique set of defined mono-, di-, and multiphosphorylated species would be observed. Although the ESI-TOF MS and rapid quench experiments reveal how many phosphorylated species are present and the relative abundance of each, the identities of each of the tyrosines phosphorylated at various reaction times were established by in-gel tryptic digestion and peptide mapping with LC/ESI-MS and MS/MS. Representative traces for peptide mapping and MS/MS sequencing are illustrated in the Supplemental Data (Figures S2 and S3).

The samples analyzed by native PAGE (Figure 1C) were digested with trypsin, and the tryptic digest was separated by reverse-phase chromatography on an Aquasil C18 column. The peptides were eluted from the column by an acetonitrile gradient and directly injected into the mass spectrometer for the MS/MS analysis. As illustrated in the third column of Figure 1D, a discrete pattern of phosphorylation in FGFR1K was determined: (1) activation loop Y653, (2) kinase insert domain Y583, (3) juxtamembrane domain Y463, (4) kinase insert domain Y585, and (5) activation loop Y654. It was found that Y653 was the only tyrosine residue phosphorylated in FGFR1K-1P; Y653 and Y583 were

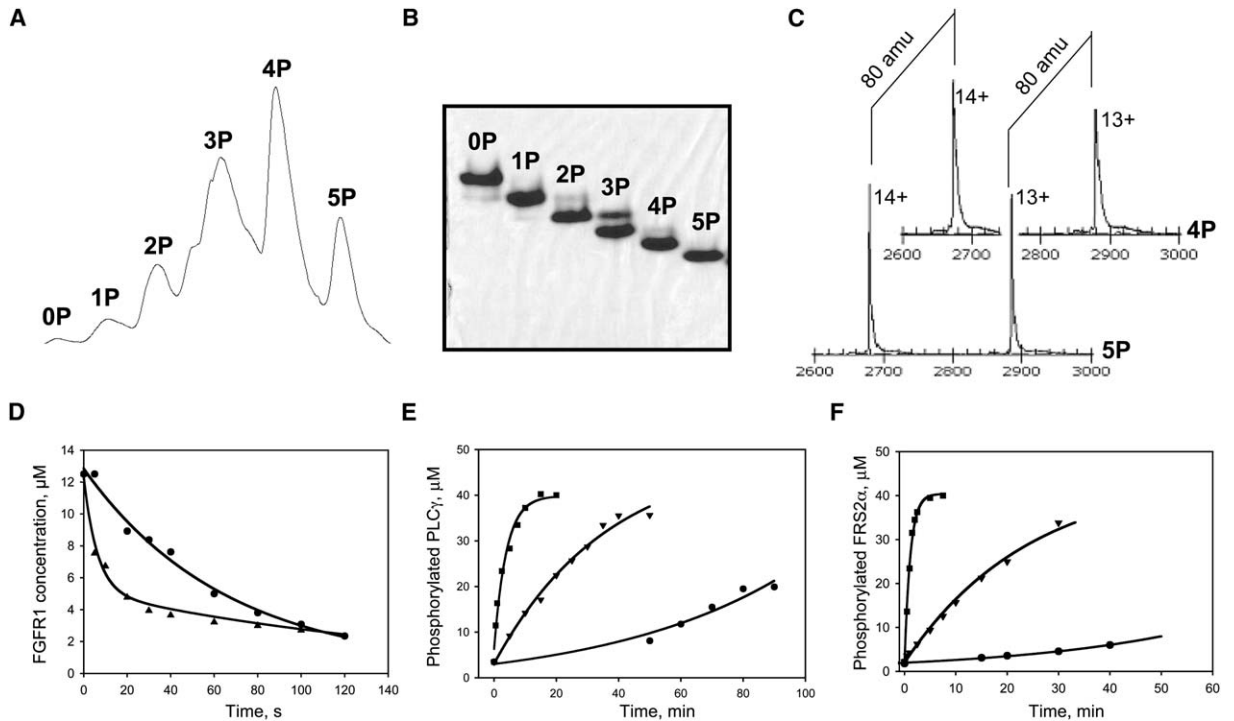


Figure 4. Two-Step Activation of FGFR1K Kinase Activity

(A–C) Summary of FGFR1K purification in different phosphorylation states. Multiple phosphorylated species of FGFR1K are separated by FPLC anion-exchange chromatography (A), and the phosphorylation state of homogeneous preparations is confirmed by native PAGE (B) and ESI-TOF MS (C).

(D) The autophosphorylation reaction of FGFR1K-0P and FGFR1K-1P was followed in the presence of 5 mM ATP and 10 mM MgCl₂. The decay of unphosphorylated (●) and monophosphorylated (▲) FGFR1K (12.5 μM) is followed as these species are converted to mono- and diphosphoryl-FGFR1K, respectively. The data were fit to exponential decay equation, and the reaction rates were 0.015 ± 0.02 s⁻¹ and 0.16 ± 0.03 s⁻¹ for the autophosphorylation of the unphosphorylated and monophosphorylated FGFR1K, respectively.

(E) Phosphorylation of recombinant PLC_γ fragment by unphosphorylated (●), mono- (▼), and diphosphorylated (■) FGFR1K-3F. The reaction rates for PLC_γ phosphorylation by the mono- and diphosphorylated FGFR1K-3F were 0.027 and 0.25 min⁻¹, respectively. The reaction rate in the presence of unphosphorylated FGFR1K-3F was estimated as <0.0005 min⁻¹.

(F) Phosphorylation of FRS2_α derived peptide by unphosphorylated (●), mono- (▼), and diphosphorylated (■) FGFR1K-3F. The reaction rates for peptide phosphorylation by the mono- and diphosphorylated FGFR1K-3F were 0.08 and 0.3 min⁻¹, respectively. The reaction rate in the presence of unphosphorylated FGFR1K-3F was estimated as <0.0005 min⁻¹. The increase in PLC_γ and peptide phosphorylation at time points higher than 40 min is most likely due to the conversion of unphosphorylated FGFR1K-3F to monophosphorylated FGFR1K-3F.

phosphorylated in FGFR1K-2P; Y653, Y583, and Y463 were phosphorylated in FGFR1K-3P; Y653, Y583, Y463, and Y585 were phosphorylated in FGFR1K-4P; and Y653, Y583, Y463, Y585, and Y654 were found to be phosphorylated in FGFR1K-5P. The complete lack of heterogeneity is quite intriguing and remarkable because there are a very large number of combinatorial possibilities (Figure 1D).

Sequential ordering of tyrosine autophosphorylation has been implicated for several receptor tyrosine kinases. For the insulin receptor (IR) and the insulin-like growth factor 1 (IGF-1) receptor, the order of tyrosine phosphorylation in the activation loop was established as Y1162, Y1158, and Y1163 in IR (Wei et al., 1995) and Y1135, Y1131, and Y1136 in IGF1R (Favelyukis et al., 2001). Also, in a separate study, it was shown that these phosphorylation events precede the phosphorylation of the C terminus tyrosine in insulin receptor (White et al., 1988). In the case of Tie2 kinase, the activation loop Y992 phosphorylation occurs prior to C terminus Y1108 phosphorylation (Murray et al., 2001). More recently, the autophosphorylation reaction of MusK tyrosine kinase was studied, and phosphorylation at Y553

in the juxtamembrane region and Y754 in the activation loop was shown to take place before phosphorylation at Y750 or Y755 (Till et al., 2002). However, these studies have not conclusively shown a discrete order of tyrosine phosphorylation beyond the tyrosines in the activation loop that are essential for kinase activation.

Having established that the tyrosine autophosphorylation of FGFR1K is a sequential and ordered process, an ancillary issue is to investigate what the kinetic and functional consequences of the phosphorylation events may be. As determined by the autophosphorylation kinetics experiments at 35 μM (Figure 3C), the rate constant for the first phosphoryl transfer was 0.05 s⁻¹ and the phosphorylation of subsequent tyrosine residues was increasingly slower. In these experiments, the amount of FGFR1K-2P is limited by the amount of FGFR1K-1P present. To accurately determine the effect of activation loop Y653 phosphorylation on catalysis, the autophosphorylation reaction was performed with monophosphorylated FGFR1K (Figure 4D). The localization of the phosphoryl group at Y653 was determined by ESI-MS/MS analysis as described above. The reaction rate of FGFR1K-2P formation was determined as

0.16 s⁻¹. This rate was 10-fold faster than the monophosphorylation rate of FGFR1K-0P (0.015 s⁻¹) when this reaction was performed under the same conditions (enzyme concentration, 12.5 μM; ATP, 5 mM).

In delineating the functional consequences of ordered, sequential phosphorylation, it is important to explore whether these features of the reaction kinetics impact downstream substrate phosphorylation. We have previously demonstrated that autophosphorylation of Y653 and Y654 is critical for tyrosine kinase activation and for phosphorylation of PLC γ , which result in recruitment and stimulation of PLC γ catalytic activity (Mohammadi et al., 1996a). The molecular mechanism of FGFR1K-mediated phosphorylation of PLC γ was next investigated by preparing a mutant form of FGFR1K containing only the two tyrosines in the activation loop (Y653 and Y654) with the three other tyrosines mutated to phenylalanines (FGFR1K-3F). Individual phosphorylated protein species of FGFR1K-3F-0P, 1P, and 2P were isolated by anion-exchange chromatography (similar to Figures 4A–4C). As illustrated in Figure 4E, the rate of phosphorylation of a PLC γ fragment with 0P, 1P, and 2P phosphorylated forms of the FGFR1K revealed that FGFR1K-1P phosphorylation of PLC γ is at least 50- to 100-fold more effective than FGFR1K-0P-mediated PLC γ phosphorylation, whereas FGFR1K-2P phosphorylates PLC γ at least 500- to 1000-fold more effectively than nonphosphorylated FGFR1K. Very similar results were obtained when a peptide derived from the docking protein FRS2 α was used as substrate for phosphorylation by the 0P, 1P, and 2P forms of FGFR1K (Figure 4F). The virtually identical results obtained in the kinetics of PLC γ fragment and FRS2 α derived peptide phosphorylation ensure that the effect observed is not due to SH2 domain-mediated recruitment by the 1P and 2P forms of FGFR1K.

An important aspect of the catalytic regulation of RTKs involves the phosphorylation of key tyrosine residues that modulate enzymatic activity and initiate downstream signal transduction to ultimately invoke a variety of metabolic changes, gene transcription, and the accompanying nuclear events. A detailed knowledge of the temporal resolution of protein signaling events has received very little attention. We have shown in this report that autophosphorylation of the catalytic kinase domain of FGFR1 is mediated by a precisely ordered reaction that results in a two-step activation process of the intrinsic catalytic activity of the FGFR1K. It is noteworthy that the fidelity of the reaction order is maintained when one or more tyrosine residues are replaced by phenylalanine residues (E.D.L., C.M.F., J.-H. Bae, K.S.A., and J.S., unpublished data). This result is consistent with the view that the high fidelity of the order of FGFR1K autophosphorylation is mediated by a precise molecular mechanism. We have compared the kinetics of phosphorylation of Y654 and other individual autophosphorylation sites when the remaining tyrosines were mutated to phenylalanines and derived similar autophosphorylation kinetics as seen with wild-type FGFR1, suggesting that the order of autophosphorylation is for the most part determined by the kinetics of phosphorylation of individual tyrosine residues in FGFR1 (E.D.L., C.M.F., J.-H. Bae, K.S.A., and J.S., unpublished data). Although we do not know whether a similarly ordered reaction takes

place in intact cells after FGF-induced stimulation of FGF-receptor autophosphorylation, the experiments presented in this report raise the possibility that the kinase activity of FGFR1 is activated in two distinct steps. After autophosphorylation of Y653 in the activation loop, which is the first tyrosine residue to be phosphorylated, the intrinsic catalytic activity of FGFR1 is enhanced, resulting in autophosphorylation of remaining autophosphorylation sites of FGFR1, some of which serve as docking sites for signaling proteins. The enhanced catalytic activity mediated by autophosphorylation of Y653 appears to be sufficient for triggering the recruitment and assembly of signaling proteins by activated FGFR1. The subsequent autophosphorylation of Y654 further enhances the catalytic activity of FGFR1 to enable efficient tyrosine phosphorylation of the assembled exogenous substrates. An important implication of this result is that the assembly of signaling molecules on FGFR1 takes place even before the catalytic activity of FGFR1 is optimally stimulated. Additional components that facilitate the assemblage of signaling molecules are SH2 and/or PTB domain-mediated associations with FGFR1 cytoplasmic domain that enhance binding affinity by reducing the K_m of substrate phosphorylation (Mohammadi et al., 1992; Hadari et al., 2001), ultimately establishing the well-coordinated, efficient, and balanced stimulation of cell signaling by activated FGFRs. The orchestration of receptor autophosphorylation, dephosphorylation, and recruitment of signaling partners may control the critical first step that initiates the kinase signal cascade and minimizes potential aberrant signaling.

Experimental Procedures

The Experimental Procedures for FGFR1K purification in unphosphorylated and phosphorylated state, native PAGE analysis, ESI-TOF MS to identify the level of FGFR1 phosphorylation, time-resolved ESI-TOF MS experiments, identification of tyrosine phosphorylation sites by ESI-LC-MS/MS, and data analysis are presented in the [Supplemental Data](#).

FGFR1K Autophosphorylation by Rapid Chemical Quench

Rapid chemical quench experiments were performed with a Kintek RFQ-3 Rapid Chemical Quench (Kintek Instruments, Austin, TX). In all cases, the concentrations of the enzyme and substrates cited in the text are those after mixing and during the reaction. The reaction was initiated by mixing the enzyme solution (15 μl) with the ATP and MgCl₂ substrates (15 μl). The reaction was quenched with 67 μl of 100 mM EDTA. The enzyme, substrates, and the quenching reagent were prepared in 10 mM HEPES buffer (pH 7.5).

The Effect of Enzyme Concentration on the Reaction Rate

In these experiments, the enzyme concentration was varied (2.5–35 μM) while the ATP and MgCl₂ concentration maintained constant (15 μl, 5 mM, and 10 mM, respectively).

The Effect of the Activation Loop Y653 Phosphorylation on the Reaction Rate

FGFR1K (12.5 μM) in unphosphorylated (0P) or monophosphorylated (1P) state was reacted with 5 mM ATP and 10 mM MgCl₂. The decay of the FGFR1K-0P and FGFR1K-1P along with the formation of FGFR1K-1P and FGFR1K-2P, respectively, was followed by quenching the reaction at different time points.

Phosphorylation of Phospholipase-C γ Fragment and FRS2 α Derived Peptide by FGFR1K

A FGFR1K construct in which all tyrosine autophosphorylation sites except Y653 and Y654 were mutated to phenylalanine was used in these experiments (FGFR1K-3F-0P). After the autophosphorylation reaction, homogeneous preparations of monophosphorylated

(pY653) and diphosphorylated species (pY653/pY654) were obtained by separating the reaction products by anion-exchange chromatography as described above. Phosphorylation of PLC γ deletion mutant (aa 541–790) and FRS2 α derived peptide (SAQRRTALL-NYENLPSLPPVWE) was followed in the presence of 0.6 μ M FGFR1-3F (in unphosphorylated, mono- or diphosphorylated states), 40 μ M PLC γ or FRS2 α derived peptide, 5 mM [γ - 32 P]ATP, and 10 mM MgCl $_2$ in 10 mM HEPES (pH 7.5). The reaction was quenched with 100 mM EDTA, the reaction mixture was separated by SDS-PAGE (10% for PLC γ experiments and 18% for FRS2 α derived peptide experiments), and the incorporation of radiolabeled phosphate in PLC γ or the peptide was monitored by phosphorimaging (Bio-Rad Molecular Imager FX).

Supplemental Data

Supplemental Data include Supplemental Experimental Procedures, three figures, and one table and can be found with this article online at <http://www.molecule.org/cgi/content/full/21/5/711/DC1/>.

Acknowledgments

We thank Jae-Hyun Bae for the phospholipase-C γ substrate. This work was supported by National Institutes of Health grants R01-GM71805 (K.S.A.), R01-AR051448 (J.S.), and R01-AR051886 (J.S.) and by funds from the Ludwig Institute for Cancer Research (J.S.).

Received: November 17, 2005

Revised: January 9, 2006

Accepted: January 18, 2006

Published: March 2, 2006

References

- Bellot, F., Crumley, G., Kaplow, J.M., Schlessinger, J., Jaye, M., and Dionne, C.A. (1991). Ligand-induced transphosphorylation between different FGF receptors. *EMBO J.* *10*, 2849–2854.
- Blagoev, B., Ong, S.E., Kratchmarova, I., and Mann, M. (2004). Temporal analysis of phosphotyrosine-dependent signaling networks by quantitative proteomics. *Nat. Biotechnol.* *22*, 1139–1145.
- Blume-Jensen, P., and Hunter, T. (2001). Oncogenic kinase signaling. *Nature* *411*, 355–365.
- Cobb, M.H., Sang, B.C., Gonzalez, R., Goldsmith, E., and Ellis, L. (1989). Autophosphorylation activates the soluble cytoplasmic domain of the insulin receptor in an intermolecular reaction. *J. Biol. Chem.* *264*, 18701–18706.
- Eswarakumar, V.P., Lax, I., and Schlessinger, J. (2005). Cellular signaling by fibroblast growth factor receptors. *Cytokine Growth Factor Rev.* *16*, 139–149.
- Favelyukis, S., Till, J.H., Hubbard, S.R., and Miller, W.T. (2001). Structure and autoregulation of the insulin-like growth factor 1 receptor kinase. *Nat. Struct. Biol.* *8*, 1058–1063.
- Grose, R., and Dickson, C. (2005). Fibroblast growth factor signaling in tumorigenesis. *Cytokine Growth Factor Rev.* *16*, 179–186.
- Hadari, Y.R., Gotoh, N., Kouhara, H., Lax, I., and Schlessinger, J. (2001). Critical role for the docking-protein FRS2 alpha in FGF receptor-mediated signal transduction pathways. *Proc. Natl. Acad. Sci. USA* *98*, 8578–8583.
- Hinsby, A.M., Olsen, J.V., Bennett, K.L., and Mann, M. (2003). Signaling initiated by overexpression of the fibroblast growth factor receptor-1 investigated by mass spectrometry. *Mol. Cell. Proteomics* *2*, 29–36.
- Honegger, A.M., Kris, R.M., Ullrich, A., and Schlessinger, J. (1989). Evidence that autophosphorylation of solubilized receptors for epidermal growth factor is mediated by intermolecular cross-phosphorylation. *Proc. Natl. Acad. Sci. USA* *86*, 925–929.
- Johnson, K.A. (2003). *Kinetic Analysis of Macromolecules*, Vol 267 (New York: Oxford University Press).
- Johnson, S.A., and Hunter, T. (2004). Phosphoproteomics finds its timing. *Nat. Biotechnol.* *22*, 1093–1094.

Li, Z., Sau, A.K., Shen, S., Whitehouse, C., Baasov, T., and Anderson, K.S. (2003). A snapshot of enzyme catalysis using electrospray ionization mass spectrometry. *J. Am. Chem. Soc.* *125*, 9938–9939.

Li, Z., Sau, A.K., Furdai, C.M., and Anderson, K.S. (2005). Probing the role of tightly bound phosphoenolpyruvate in Escherichia coli 3-deoxy-d-manno-octulosonate 8-phosphate synthase catalysis using quantitative time-resolved electrospray ionization mass spectrometry in the millisecond time range. *Anal. Biochem.* *343*, 35–47.

Mohammadi, M., Honegger, A.M., Rotin, D., Fischer, R., Bellot, F., Li, W., Dionne, C.A., Jaye, M., Rubinstein, M., and Schlessinger, J. (1991). A tyrosine-phosphorylated carboxy-terminal peptide of the fibroblast growth factor receptor (Fig) is a binding site for the SH2 domain of phospholipase C-gamma 1. *Mol. Cell. Biol.* *11*, 5068–5078.

Mohammadi, M., Dionne, C.A., Li, W., Li, N., Spivak, T., Honegger, A.M., Jaye, M., and Schlessinger, J. (1992). Point mutation in FGF receptor eliminates phosphatidylinositol hydrolysis without affecting mitogenesis. *Nature* *358*, 681–684.

Mohammadi, M., Dikic, I., Sorokin, A., Burgess, W.H., Jaye, M., and Schlessinger, J. (1996a). Identification of six novel autophosphorylation sites on fibroblast growth factor receptor 1 and elucidation of their importance in receptor activation and signal transduction. *Mol. Cell. Biol.* *16*, 977–989.

Mohammadi, M., Schlessinger, J., and Hubbard, S.R. (1996b). Structure of the FGF receptor tyrosine kinase domain reveals a novel autoinhibitory mechanism. *Cell* *86*, 577–587.

Murray, B.W., Padriquet, E.S., Pinko, C., and McTigue, M.A. (2001). Mechanistic effects of autophosphorylation on receptor tyrosine kinase catalysis: enzymatic characterization of Tie2 and phospho-Tie2. *Biochemistry* *40*, 10243–10253.

Parast, C.V., Mroczkowski, B., Pinko, C., Misialek, S., Khambatta, G., and Appelt, K. (1998). Characterization and kinetic mechanism of catalytic domain of human vascular endothelial growth factor receptor-2 tyrosine kinase (VEGFR2 TK), a key enzyme in angiogenesis. *Biochemistry* *37*, 16788–16801.

Pawson, T., and Nash, P. (2003). Assembly of cell regulatory systems through protein interaction domains. *Science* *300*, 445–452.

Schlessinger, J. (2000). Cell signaling by receptor tyrosine kinases. *Cell* *103*, 211–225.

Steen, H., Kuster, B., Fernandez, M., Pandey, A., and Mann, M. (2002). Tyrosine phosphorylation mapping of the epidermal growth factor receptor signaling pathway. *J. Biol. Chem.* *277*, 1031–1039.

Till, J.H., Becerra, M., Watty, A., Lu, Y., Ma, Y., Neubert, T.A., Burden, S.J., and Hubbard, S.R. (2002). Crystal structure of the MuSK tyrosine kinase: insights into receptor autoregulation. *Structure* *10*, 1187–1196.

Wei, L., Hubbard, S.R., Hendrickson, W.A., and Ellis, L. (1995). Expression, characterization, and crystallization of the catalytic core of the human insulin receptor protein-tyrosine kinase domain. *J. Biol. Chem.* *270*, 8122–8130.

White, M.F., Shoelson, S.E., Keutmann, H., and Kahn, C.R. (1988). A cascade of tyrosine autophosphorylation in the beta-subunit activates the phosphotransferase of the insulin receptor. *J. Biol. Chem.* *263*, 2969–2980.

Yarden, Y., and Schlessinger, J. (1987a). Epidermal growth factor induces rapid, reversible aggregation of the purified epidermal growth factor receptor. *Biochemistry* *26*, 1443–1451.

Yarden, Y., and Schlessinger, J. (1987b). Self-phosphorylation of epidermal growth factor receptor: evidence for a model of intermolecular allosteric activation. *Biochemistry* *26*, 1434–1442.

Zhang, Y., Wolf-Yadlin, A., Ross, P.L., Pappin, D.J., Rush, J., Lauffenburger, D.A., and White, F.M. (2005). Time-resolved mass spectrometry of tyrosine phosphorylation sites in the EGF receptor signaling network reveals dynamic modules. *Mol. Cell. Proteomics* *4*, 1240–1250.